International Journal of Applied and Advanced Scientific Research (IJAASR)
Impact Factor: 5.655, ISSN (Online): 2456 - 3080
(www.dvpublication.com) Volume 8, Issue 2, 2023

GRAPHENE-BASED AU TIO2 TERM NANO COMPOSITES FOR PHOTOCATALYTIC APPLICATIONS

Aditi Kumari
Department of Chemistry (NET Qualified), MDU Rohtak, Haryana

Cite This Article: Aditi Kumari, "Graphene-Based Au Tio2 Term Nano Composites for Photocatalytic Applications", International Journal of Applied and Advanced Scientific Research, Volume 8, Issue 2, July - December, Page Number 21-26, 2023.

Abstract:

This study provides an overview of photocatalysts and their history, as well as information on their fundamentals, the photocatalytic process, and the thermodynamics of the photocatalytic process. Selection criteria, material qualities, and potential uses for the three materials (TiO2, graphene, and gold) have also been explored. The results reveal that although pure TiO2 has a negligible MB dye degradation efficiency in a dark media, a rGO1-TiO2 photocatalyst has a very high one. The results also show that the addition of graphene oxide enhances the TiO2's efficacy in degrading MB dye. The MB dye is degraded by the rGO1-TiO2 photocatalyst by about 60% in dark media. Degradation and mineralization of MB dye may be seen in 105 minutes when TiO2 is present under illumination. In contrast, rGO1-TiO2 photocatalysts rapidly deteriorate after 60 minutes. Hence, only rGO1-TiO2 was subjected to further Au loading. When comparing the photo-catalytic activity of the various produced catalysts, A2rGO-TiO2 (with 2.0 wt% of Au) stands out as having the highest rate, with about 95% of MB degraded after 45 minutes.

Key Words: Graphene, Au, TiO_2, Ternary Nano Composites, Photo catalytic Applications.

Introduction:

The simple definition of photo-catalysis is the acceleration of a chemical reaction by the presence of a catalyst that attracts light and incorporates it into the reaction process. Light is absorbed to generate electron (e) -hole (h), i.e., charge-pairs; the excited charge-carriers are dissociated; electrons and holes are moved to the surface/interface of the photo catalysts; and the charges populated there are used in redox reactions. When it comes to the third phase, it's common for a lot of electron-hole pairs to interact on their way to the surface or after they get at the surface's active sites. Both non-radiative recombination (as heat) and radiative recombination (as light) contribute to the energy's loss during the recombination/interaction (as a form of light emission). Depending on the donor/acceptor features of the surface-captured species, the photo-generated charge pairs on the surface-interface of the catalysts may induce various reduction-oxidation events.

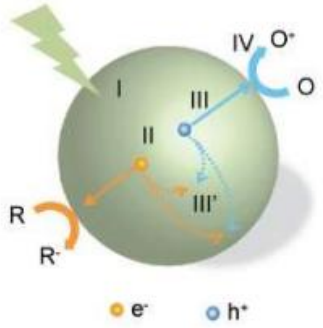

Figure 1: Steps involved in the photo-catalytic reaction process {R represents reductive chemicals reactions; O: represents oxidative chemicals reactions}

Materials Selection for Hetero-Nanostructure Photocatalysts Designing:

The fabrication of new photo-catalytic materials with improved properties is greatly aided by hetero structured photo-catalytic materials may also fulfil kinetic and thermodynamic stability. Heterostructured materials that absorb light may offer the necessary band gap for maximising production yield. As a result, constructing the hetero-nanostructure for better and efficient photocatalytic application, including photocatalytic water splitting, hydrogen evolution, and the breakdown and mineralization of pollutant dyes, requires careful consideration of the materials available. TiO2 semiconductor, Graphene oxide, and Gold were selected as the building blocks for the creation of novel ternary photocatalysts (Au). The following is a synopsis of these resources.

Titanium Dioxide (TiO2):

Titanium dioxide (TiO2) occurs in nature in three distinct forms: anatase, brookite, and rutile. Although while all these TiO2 polymorphs are quite clean, they do have some detectable impurities that give them a dingy hue. These impurities may be traced back to elements like iron, chromium, or vanadium. Consequently, the purification is necessary before it may be used in any practical context. The thermodynamically stable phase of TiO2 is rutile, whereas the other two polymorphs are metastable. Due to the abundance of crystallographic data on its many polymorphs, titanium dioxide has been elevated to the status of a leading candidate for the most

significant titanium oxide. To be more specific, the anatase and rutile polymorphs of TiO2 are the most widely utilised and economically manufactured forms from a technological standpoint.

- The mineral srilankite, often known as TiO2, is an orthorhombic homologue of the lead oxide
- a variant of the form cubic fluorite
- Polymorph of the pyrite mineral
- Polymorphism of the monoclinic baddeleyite type
- Polymorph of the cotunnite kind

In terms of research and development operations, these polymorphs do not have as much significance.

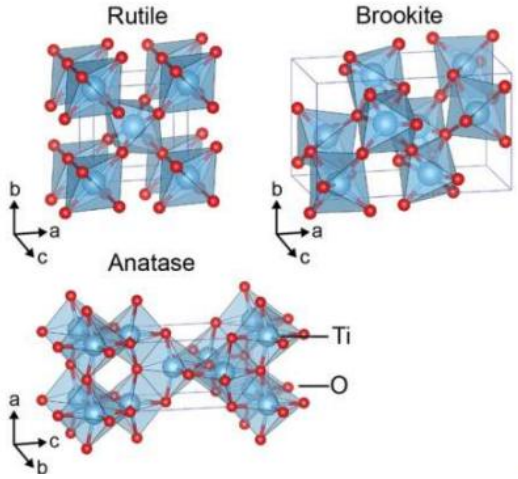

Figure 2: Crystal structure of titanium dioxide (TiO2) rutile (tetragonal, P42/mnm), brookite (orthorhombic, Pbca) and anatase (tetragonal I41/amd) polymorphs [64]

Graphene Oxide:

Graphene is a two-dimensional sheet of carbon molecules that is just one atom thick and has a honeycomb-like sp2 bonding and packing structure. Graphene is the basic material from which graphite, nanostructures, and fullerenes are constructed. In Fig. 1.3 we see the several carbon allotropes that exist. In 1940, its theoretical role as a component of graphite was established. By heating and chemically reducing graphite oxide, Boehm et al. in 1962 were able to isolate a single layer of carbon and discover that it was thermodynamically unstable at room temperature. The development of single layers of graphene by Geim et al. in 2004 opened up new avenues of inquiry in the domains of physics, chemistry, biology, and materials science. Graphene, the "thinnest" known carbon allotrope, has remarkable properties like low coefficient of thermal expansion (CTE), high thermal conductivity, low thermal expansion coefficient, and high electrical conductivity. Graphene's special properties have sparked intense attention from scientists and businesspeople alike.

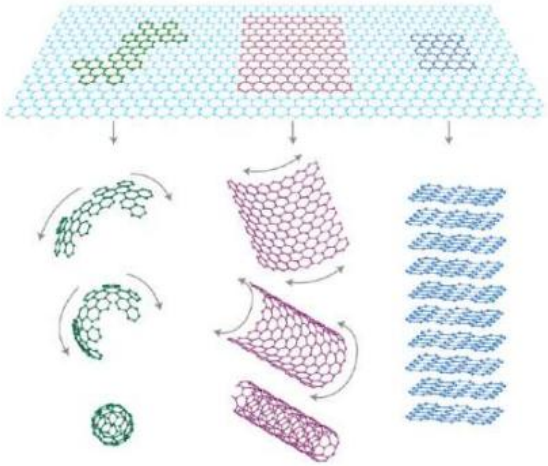

Figure 3: All form of graphite, i.e., Graphene, Nanotube and fullerene

Plasmonic Gold as Co-Catalyst:

In light of their low optical loss over a broad photo-spectrum, noble metals like silver (Ag), gold (Au), copper (Cu), palladium (Pd), etc. are regarded as ideal possibilities for surface plasmon resonance (SPR) applications. It has been first investigated for plasmonic applications because to its unusually low optical loss of Ag in the visible and near Infrared area, and it was shown to exhibit the SPR features. Nevertheless, its

usefulness in optical applications is limited by the rapid surface oxidation tendency, which tends to cause optical loss. Gold, on the other hand, was recognised as a possible material for SPR applications owing to its remarkable chemical stability in ambient conditions and its possession of shared plasmonic property with Ag in the visible and near Infrared range. Yet, their usefulness is limited by their high price tag. Copper and aluminium have been considered as a potential low-cost SPR material option. They are chemically unstable under ambient conditions, limiting their usefulness as a co-catalyst for optical response.

In addition, scientists have investigated alkali materials and discovered that they, too, exhibit plasmonic characteristics and may be excellent options for plasmonic applications. They are very reactive to oxygen and water, thus they must be stored in a vacuum or an inert gas environment, which poses a considerable issue for their long-term stability. As a result, materials from the alkali group saw limited usage in plasmonics. Despite their low plasmonic sensitivity, Pd and Pt have attracted considerable interest for usage in photocatalytic applications because to their significant absorption of visible light.

Methods and Materials:

Synthesis of GO, TiO2, rGO-TiO2, and Au-loaded rGO-TiO2 Photocatalysts: An Experimental Approach

Materials:

" The precursor materials such Graphite powder (325 mesh, Alfa aeser), Hydrochloric acid (HCl, 37%, Fisher), Sulfuric acid (H2SO4, Fisher 98%, AR), Potassium permanganate (KMnO4, Fisher), Hydrogen peroxide (H2O2, 30%, AR), and Tetra-isopropoxide (TTIP, Merck), hydrogen tetrachloroaurate (III) hydrate (HAuCl4.H2O, 99.9%, Aldrich), ethyl alcohol (EtOH, 95% , Merck) procured for the preparation of hetero-nanostructure photocatalysts were used as received without further purification".

Synthesis procedure of Graphene Oxide (GO):

The flow chart for the synthesis process is illustrated in Figure 3.1. Graphene oxide sheets (GOs) were made by following Hummer's technique with slight changes and then utilising commercial natural graphite powder as the starting material. A standard approach called for placing 18 mL of concentrated sulfuric acid (H2SO4) in a beaker that held 100 mL of liquid. After that, 2.0 grammes of sodium nitrate (NaNO3) and 0.5 grammes of graphite powder were added to the solution of H2SO4, and the whole mixture was agitated vigorously for one hour at a temperature of 0 degrees Celsius in an ice bath.

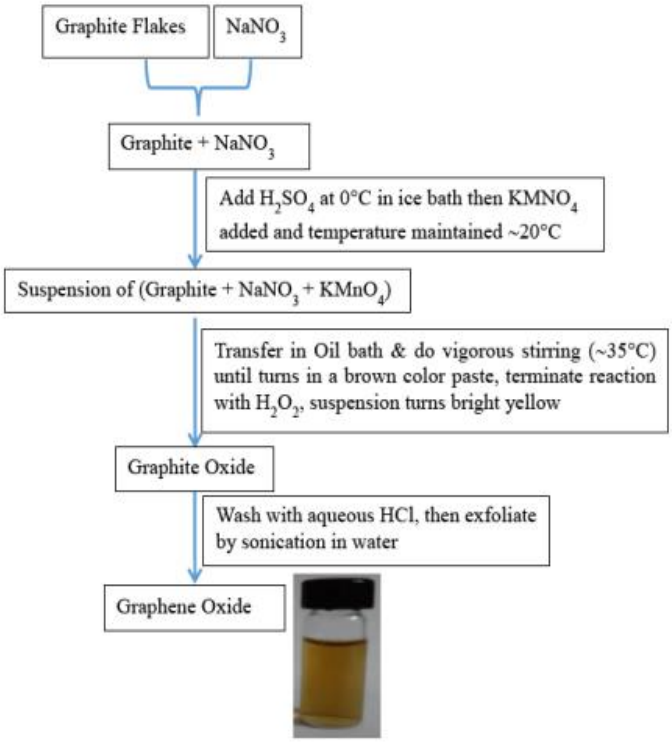

Figure 4: Flow-chart for the synthesis of graphene oxide by Hammer's method

After that, a total of 3.0 grammes of potassium permanganate (KMnO4) powder was gradually added to the previously combined solution, and the whole combination was agitated consistently for a period of three hours. The combination was discovered to produce a paste of a dark brown tint. In the next stage, following a stepwise addition method, 110 mL of deionized water with a conductivity of 18.4 M cm and 10 mL of H2O2 with a concentration of less than 30% were added to the mixture that was previously created. The whole solution

combination became a dispersion that had a yellowish hue, and it was washed many times with a solution of diluted hydrochloric acid and water in order to get rid of any insoluble salt.

Synthesis of TiO2 Nanoparticles:

An environmentally friendly sol-gel process was used to produce TiO2 nanoparticles. Initial components were titanium tetra-isopropoxide (TTIP), ethyl alcohol, and hydrochloric acid (HCl). Drop by drop, 0.5 mL of HCl (37% v/v) was added to 20 mL of ethanol in a beaker. Ten minutes were spent stirring the whole batch. The above solution was then gently added to 2.5 mL TTIP. After 4 hours of stirring, the solution had the consistency of a clear gel made of TiO2. After 12 hours at 100 degrees Celsius, the TiO2-gel was dried in a hot air oven. The solid TiO2 thus produced was next mechanically ground and calcined in a muffle furnace at 450°C for 1 hour. The samples were collected and placed in an airtight container (flushed with nitrogen).

Synthesis of (rGO)-TiO2 Binary Hetero-Nanostructure Photo-Catalysts:

Figure 4 is a flowchart depicting the production of reduced graphene oxide (rGO)-TiO2, a binary hetero-structured photo catalyst generated by a hydrothermal procedure. In order to enhance exfoliation, GOs was suspended in a water-ethanol (2:1) mixture for 24 hours. After 2 hours of ultra-sonication, the aqueous GOs suspension was re-exfoliated in a solution of water and ethanol (2:1). To achieve a uniform dispersion of the components, 1 g of TiO2 powder was added to an aqueous solution of re-exfoliated GOs, and the mixture was stirred gently for 2 hours. Then, a 100 mL Teflon-sealed autoclave was used to hydrothermally treat 60 mL of the homogenous solution. To perform the hydrothermal therapy, temperatures were maintained at 180 degrees Celsius for 5 hours. For rGO-TiO2 to develop, the hydrothermal treatment method must allow TiO2 to bind to the rGO's active sites. Attaching rGO-TiO2 nano composites is shown in a simplified form in Scheme 3.1.

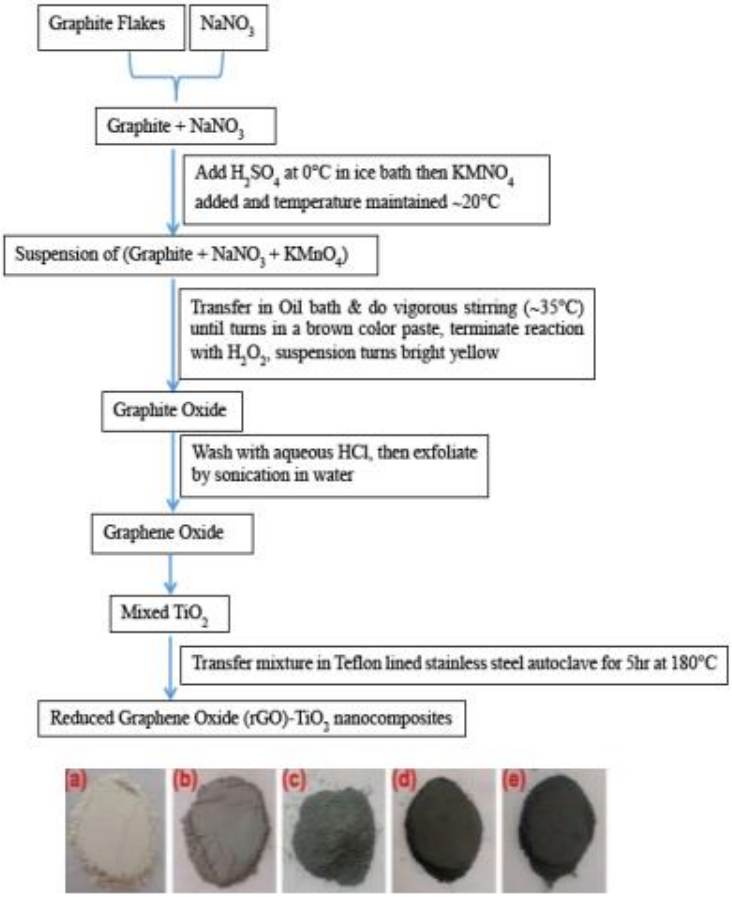

Figure 5: Flow-chart for the synthesis of rGO-TiO2 nanocomposites. Digital images of (a) bare TiO2; TiO2 with rGO [(b) 0.5 wt%, (c) 1.0 wt% (d) 2.0 wt% and (e) 4.0 wt%]

The hetero-structured composite was reclaimed by first washing the material with ethanol and then rinsing it many times in deionized water. This process was repeated until the desired consistency was reached. The substance, which was given the designation reduced graphene oxide - titanium dioxide (rGO - TiO2), was dried in an oven at a temperature of 40 degrees Celsius for a period of 12 hours. During the procedure, TiO2 with varying weight percentages of graphene oxide (e.g., 0.5, 1.0, 2.0, and 4.0 wt%) was synthesised for use in further research. The samples have been given the names reduced graphene oxide rGOX-TiO2 (where X = 0.5, 1.0, 2.0, and 4.0 weight%), which translates to rGO0.5-TiO2, rGO1-TiO2, rGO2-TiO2, and rGO4-TiO2, respectively. The basic steps involved in the production of rGO-TiO2 nano composite are outlined in Scheme 3.1.

Result and Discussion:

Phase Analysis of GO, TiO2, rGO-TiO2 and Au Loaded rGO-TiO2:

Anatase and rutile are the two structural phases of TiO2 that have been seen in XRD patterns of pure TiO2 samples. Based on the dhkl values, the lattice parameters for the anatas phase are a = 0.3726 nm and c = 0.9943 nm, whereas those for the rutile phase are a = 0.4604 nm and c = 0.2967 nm (interplanar spacing). Density = 3.84 g/cm3 for anatas and 4.25 g/cm3 for rutile are obtained from their respective unit cell volumes Vo = 0.0629 nm3 and 0.1380 nm3, respectively. The elimination of the GO peak in the presence of rGO-TiO2 nano-composite is indicative of the successful conversion of graphene oxide to its reduced form (rGO). The impact of Au loading on the phase structure of TiO2 nanoparticles was also investigated using the XRD patterns. None of the peak locations changed noticeably after Au loading, suggesting that Au loading had little effect on the crystalline phase composition of the TiO2. There is no evidence of alteration of the original TiO2 structure after Au loading of 0.5 to 5.0 wt%, with only a significant augmentation in the intensity of (110) peak reflection. We calculated average crystallite sizes to be 25, 23.2, 20.5, 18.6, and 15.3 nm for TiO2, rGO1-TiO2, A0.5rGO1-TiO2, A1rGO1-TiO2, and A5rGO1-TiO2 ternary nanocomposites photo-catalysts. As Au nanoparticles loading limit the formation of TiO2 nanocrystals by creating different borders and hindering the mass transportation, the average crystallite sizes are shown to drop somewhat with Au loading, demonstrating that the Au presence effects crystallite size.

Microstructural Analysis of GO, TiO2, rGO-TiO2 and Au Loaded rGO-TiO2:

Scanning and Transmission Electron Microscopes (SEM and TEM) were used to analyse the morphology of the produced materials (TEM). The TiO2 nanoparticles on rGO's surface are discovered to be rather tiny and highly aggregated. TEM pictures of GO and its composite samples reveal locally crumpled GO-sheet, which may be a result of a variation in the nucleation growth rate of particles. The particle size distribution of TiO2 nanoparticles is rather narrow, between 20 and 30 nm. Yet, it is also shown that the TiO2 nanoparticles create a composite structure by being tightly bound to the rGO surface. This interfacial contact and preferred heterogeneous nucleation agglomerate in a specific area due to the presence of hydrophilic functional groups and hydroxyl groups, which have a distinct nucleation growth rate. As these two materials are so close together, electrons may easily be transferred from the TiO2 nanoparticles to the graphene sheets when they are photo-excited.

In addition, Figure 4's SEM pictures of as-prepared Au loaded rGO1-TiO2 samples demonstrate the uniform distribution of Au particles over the rGO1-TiO2 surface. The TEM picture of an Au-loaded rGO1-TiO2 sample reveals that the metal particles, which range in size from around 5 to 10 nm, deposit on the TiO2 irregular thin platelet structure with a sphere-like shape. In order to learn more about the rGO, Au, and TiO2 components of the ternary nanocomposites A2rGO1-TiO2, we additionally gathered a high-angle annular dark-field scanning transmission electron microscopy (HAADF STEM) picture and elemental mapping data. EDS analysis of Au loaded rGO1-TiO2 ternary nanocomposites reveals the presence of Carbon, Gold, Oxygen, and Titanium.

X-Ray Photoelectron Spectroscopy for Surface / Interface Elemental Analysis:

The chemical composition of a material's surface may be revealed via X-ray photoelectron spectroscopy (XPS). Ti (Ti2p), O (O1s), and C (C1s) peaks are prominent in the whole survey spectrum of rGO(1 wt%) with TiO2. Graphite oxidation into GO was inferred from the observation that oxygenated carbon had a higher peak intensity than C-C. Peak binding energies of 284.1, 286.2, and 287.6 eV are discovered for the C-C, C-OH, and C=O species in GO, respectively. The existence of residual oxygenated groups may account for similar peaks seen in rGO-TiO2. The existence of Ti4+, as shown by the high resolution Ti (2p) spectra, indicates that the TiO2 crystal structure was preserved. TiO2's O-Ti bond was given the bands at binding energies of 457.9 eV (Ti 2p3/2) and 463.8 eV (Ti 2p1/2).

“ Strong Ti (Ti2p), O (O1s), C (C1s), and Au (Au4f) peaks can be seen in the whole survey spectrum of Au (2.0 wt%) loaded rGO (1.0 wt%)-TiO2, i.e., A2rGO1-TiO2 ternary nanocomposites in Fig. 5.7. The Au loading on rGO-TiO2 is supported by the presence of Au, C, O, and Ti in survey spectra. Reduced graphene oxide (rGO) was detected when the C-C/C=C peak intensity was higher than that of the C=O and C-OH peaks. Binding energies of 284.07, 285.48 and 285.8 eV are detected for the C-C, C=O, and C-OH peaks in GO, respectively. The existence of Ti4+ in a high-resolution Ti (2p) spectrum suggests that TiO2's crystal structure was preserved throughout the reaction. Bands at 457.9 eV (Ti 2p3/2) and 463.8 eV (Ti 2p1/2) were identified as belonging to the O-Ti bond in TiO2. The existence of Au bands at 86.78 eV (Au 4f5/2) and 82.95 eV (Au 4f7/2) in a high-resolution Au (4f) spectra indicates that these binding energies are present”.

Conclusion:

Briefly mentioned here are some of the most significant results and implications of this study.

- Powdered photo-catalysts made from synthesised GO, TiO2, rGO-TiO2, and Au-loaded rGO-TiO2 were characterised and fabricated.
- The X-ray diffraction pattern reveals that the TiO2 is composed of two distinct structural phases: anatase and rutile. Based on the dhkl values, the lattice parameters for the anatas phase are a = 0.3726

nm and c = 0.9943 nm, whereas those for the rutile phase are a = 0.4604 nm and c = 0.2967 nm (interplanar spacing). The densities = 3.84 g/cm3 and 4.25 g/cm3 are obtained from the unit cell volumes Vo = 0.1380 nm3 and 0.0629 nm3, respectively.

- In TEM. We find that the TiO2 nanoparticles agglomerate on the surface of rGO-sheets and are rather tiny in size. The GO-sheet has several wrinkles in it. Using transmission electron microscopy, we can see that the metal Au particles in the rGO1.0-TiO2 sample have a spherical shape, which is deposited on the uneven thin platelet structure of the TiO2. Carbon, gold, oxygen, and titanium can all be seen in EDS maps and high-angle annular dark-field scanning TEM (HAADF-STEM) images of Au-loaded rGO-TiO2 ternary nanocomposites.
- "Typical D-band at 1340 cm-1 and peak at 1610 cm-1, referred to as G - band, can be seen in the Raman spectra of GO samples. Pure TiO2 has Raman bands at 143, 144, 235, 395, 445, 515, 612, and 638 cm-1, all of which are associated with characteristic TiO2 vibrational modes. Anatase-TiO2 phase is responsible for the appearance of peaks at 143, 395, 515, and 638 cm-1, which are associated with the Eg(1), B1g(1), A1g + B1g(2), and Eg(2) modes of vibration, respectively. B1g, two-phonon scattering, Eg, and A1g modes of vibration in the rutile- TiO2 phase account for the peaks at 144, 235, 445, and 612 cm-1, respectively.
- In rGO-TiO2 composites, the D and G-band peaks of graphene were observed to be relocated from their typical locations. TiO2 is effectively integrated in GO sheets to create rGO- TiO2 composite material, as shown by an increase in the D/G intensity ratio from 1.18 (in the case of 0.5 wt% GO) to 1.24 (in the case of 1 wt% GO) and 1.27 (in the case of 2 wt% GO). Raman active modes of vibration show that TiO2's intensity is diminished when GO is incorporated into the molecule, with the replacement of one or more -bonds. The addition of Au nanoparticles to rGO-TiO2 increases the TiO2 peak intensity by around 690%, while the D and G peaks increase in intensity by over 400%. The reason for this is because Au nanostructures create localised surface plasmon resonance. Loading Au on the rGO surface did not, however, cause any structural changes in the rGO, as shown by the fact that the relative intensity ratio of the D and G peaks (ID/IG) remained unaffected".
- TiO2 doped with 1 wt% GO had the highest absorption rates. An increase in electron density at the material's surface, as shown by a rise in absorption intensity, is conducive to efficient electron transfer. The calculated band gap energy for TiO2 with 0.5 wt% rGO included changes from 3.12 eV (for TiO2) to 2.89 eV (for rGO-TiO2). In the case of 2 wt% rGO-TiO2, the band gap shifts to 2.99 eV. The development of Ti-C covalent bonds in the case of rGO-TiO2 nano-composites (with varying wt% of rGO) may be connected to the narrowing of the band gap.

References:

1. A. Albini and M. Fagnoni, "1908: Giacomo ciamician and the concept of green chemistry," Chem Sus Chem, vol. 1, no. 1-2, pp. 63-66, 2008.
2. M. B. Tahir, M. Rafique, M. Sagir, S. Ullah, and H. Kiran, "Nanomaterials for Photocatalytic Applications," Ref. Modul. Mater. Sci. Mater. Eng., 2019.
3. K. J. Balkus, Metal Oxide Nanotube, Nanorod, and Quantum Dot Photocatalysis. Catalysis by Nanopsrtices, 2013.
4. U. Koch, A. Fojtik, H. Weller, and A. Henglein, "Photochemistry of semiconductor colloids. Preparation of extremely small ZnO particles, fluorescence phenomena and size quantization effects," Chem. Phys. Lett., vol. 122, no. 5, pp. 507-510, 1985.
5. S. E. Braslavsky and M. B. Rubin, "The history of ozone: Part VIII. Photochemical formation of ozone" Photochem. Photobiol. Sci., vol. 10, no. 10, pp. 1515-1520, 2011.
6. A. Fujishima, X. Zhang, and D. A. Tryk, "TiO2 photocatalysis and related surface phenomena," Surf. Sci. Rep., vol. 63, no. 12, pp. 515-582, 2008.
7. K. K. Andreew and J. B. Chariton "The Mechanism of Self-Propagating Chain," Trans. Faraday Soc., Vol. 31, pp. 797-804, 1935.
8. P. Lotfabadi, "Analyzing passive solar strategies in the case of high-rise building," Renew. Sustain. Energy Rev., vol. 52, pp. 1340-1353, 2015.
9. D. Ravelli, D. Dondi, M. Fagnoni, and A. Albini, "Photocatalysis. A multifaceted concept for green chemistry," Chem. Soc. Rev., vol. 38, no. 7, pp. 1999- 2011, 2009.
10. C. Panagopoulos and H. Badekas, "Electronic system conduction in The Ti/TiO/electrolyte," J. of the Less Common Metals, Volume 133, no. 2, pp. 245- 253,1987.
11. P. J. Boddy, "Oxygen Evolution on Semiconducting TiO2," J. Electrochem. Soc., vol. 115, no. 2 115, pp. 199-203, 1968.
12. L. Finegold and J. L. Cude, "Biological sciences: One and two-dimensional structure of alpha-helix and beta-sheet forms of poly(L-Alanine) shown by specific heat measurements at low temperatures (1.5-20 K)," Nature, vol. 238